Materials Science & Engineering A 642 (2015) 391–397

Contents lists available at ScienceDirect

Materials Science & Engineering A

journal homepage: www.elsevier.com/locate/msea

Comparison of crack resistance between ternary CrSiC and quaternary CrSiCN coatings via nanoindentation

Qianzhi Wang [a], Zhiwei Wu [b,c], Fei Zhou [b,c,*], Jiwang Yan [a,**]

[a] Department of Mechanical Engineering, Faculty of Science and Technology, Keio University, Yokohama 2238522, Japan
[b] College of Mechanical and Electrical Engineering, Nanjing University of Aeronautics and Astronautics, Nanjing 210016, China
[c] Jiangsu Key Laboratory of Precision and Micro-Manufacturing Technology, Nanjing 210016, China

ARTICLE INFO

Article history:
Received 3 June 2015
Accepted 9 July 2015
Available online 10 July 2015

Keywords:
PVD coatings
Nanoindentation
Crack
Residual stress
Morphology

ABSTRACT

Quaternary CrSiCN and ternary CrSiC coatings with various Si concentrations were synthesized on Si (100) wafers via adjusting the flow of $(CH_3)_3SiH$ (TMS) in precursor gases. The mechanical property and crack resistance of these coatings were evaluated and compared, as well as the influence of Si concentration was investigated. Compared with the CrSiC coatings, the CrSiCN coatings had higher elasticity and compressive stresses, and in turn, exhibited higher resistance to radial cracks in despite of the Si concentration. The greater thickness of CrSiCN coatings is, the better the crack resistance is. By increasing Si concentration, the compressive stress was released in both categories of coatings, but the trends of crack generation for the two categories of coatings were totally different. For the CrSiCN coatings, a reduction of compressive stress prevented parallel crack initiation around the impression edge after unloading. In contrast, as the compressive stress in the CrSiC coatings was released, radial cracks were generated at the impression corners and the length of radial crack increases with the stress release.

© 2015 Elsevier B.V. All rights reserved.

1. Introduction

Silicon nitride (SiN_x) is a promising material for wear protection coatings due to its excellent strength and hardness, low thermal expansion, and durability [1–4]. Thereby, in order to meet growing requirement in industry for superior coatings with good mechanical and tribological properties, academic circles have concentrated on building a composite architecture of nano-crystal dispersing into amorphous SiN_x matrix [5–28]. One of the most common ways is to introduce Si element into transition metal-based coatings such as TiN [6–12], CrN [13–19], ZrN [20], MoN [21], TaN [22], TiCN [23–25] and CrCN [26–28]. For instance, TiSiN coatings presented high hardness over 30 GPa due to refined grain, compact microstructure and a nano-composite architecture after Si addition [9–11]. As a result, long service life was obtained when TiSiN coatings were applied on cutting tools [6,7]. Likewise, with Si alloying, CrSiN coatings became harder than CrN coatings [13–16], and therefore, the friction coefficient and wear rate of tribopair decreased from 0.55 to 0.4 and from 11.0×10^{-7} mm^3/Nm to 5.0×10^{-7} mm^3/Nm, respectively [19]. All the above-mentioned literature indicates that amorphous SiN_x in ternary TiSiN and CrSiN coatings plays an extremely important role in enhancing their mechanical and tribological properties.

As we know, TiCN and CrCN coatings, as potential candidates for TiN and CrN coatings, have attracted researchers' attention for many years due to a combination of hard phase of TiN(CrC) and self-lubrication effect of carbon. However, Fuentes et al. [29] and Warcholinski's group [30–33] pointed out that the residual stress of CrCN coatings was more intensive than CrN coatings, as well as rougher surface. On the other hand, higher density of surface particle, more defects and worse adhesion of TiCN coatings after C doping were reported in Refs. [34,35]. Thus, Si element, which shows positive effect on improving mechanical properties of TiN and CrN coatings, draws researchers' focus again. Kuptsov et al. [23] pointed out that the hardness of TiSiCN coatings increased to 42.9 GPa with 12 at% Si addition, and presented superior impact resistance. In addition, the surface refinement of CrCN coatings by doping Si were reported in Refs. [26,27]. However, previous investigations either studied corrosion behavior alone [26,27], or focused on a specific Si concentration [23,36,37]. So far, there is no systematic research to compare CrSiC with CrSiCN to investigate the advantage of N alloying, as well as the influence of Si concentration on the residual stress, mechanical property and crack resistance of these coatings.

In this study, the microstructure, residual stress, mechanical property and crack resistance of CrSiC and CrSiCN coatings with various Si concentrations were investigated by using X-ray

* Corresponding author. Tel/fax.: +86 25 8489 3083.
** Corresponding author. Tel.: +81 45 566 1445; fax: +81 45 566 1495.
E-mail addresses: fzhou@nuaa.edu.cn (F. Zhou), yan@mech.keio.ac.jp (J. Yan).

http://dx.doi.org/10.1016/j.msea.2015.07.024
0921-5093/© 2015 Elsevier B.V. All rights reserved.

diffraction (XRD), white-light interferometer, nanoindentation and field-emission scanning electron microscope (FE-SEM). Through a comparison of the experimental results, the correlation among the microstructure, the mechanical property and the crack resistance of the coatings was elucidated.

2. Experimental details

2.1. Fabrication of coatings

By using closed-field unbalanced magnetron sputtering system (UDP-650, Teer Coatings Limited, UK), ternary CrSiC and quaternary CrSiCN coatings were fabricated on Si(100) wafers, which were fixed on turning holder after ultrasonic bath in ethanol and deionized water. Prior to deposition, a 30 min. Ar^+ bombardment at bias voltage of −450 V was performed to remove contamination from substrate. After this process, a Cr interlayer with thickness of 0.4 μm was deposited on Si wafer beforehand to enhance the adhesion between substrate and top coating. Subsequently, CrSiC coatings were fabricated by sputtering one Cr target (4.0 A) and one C target (1.0 A) in precursor gases (TMS and Ar). CrSiCN coatings were fabricated by sputtering one Cr target (4.0 A) in precursor gases (TMS, N_2 and Ar). During deposition, the rotating speed of holder, bias voltage and OEM were set as 10 rpm, −80 V and 50%, respectively. Via adjusting the flow of TMS from 10 sccm to 30 sccm, CrSiC and CrSiCN coatings with various Si concentrations were obtained. The symbols of CrSiC(10), CrSiC(20), CrSiC (30), CrSiCN(10), CrSiCN(20) and CrSiCN(30) will be cited to denote coatings deposited under different TMS flows in the next sections.

Table 1
Thickness and element concentration of CrSiCN and CrSiC coatings at different TMS flows.

Coatings	Thickness (μm)	Cr (at%)	Si (at%)	C (at%)	N (at%)
CrSiCN(10)	2.23	40.02	2.67	10.68	46.63
CrSiCN(20)	2.10	47.76	5.53	14.98	31.73
CrSiCN(30)	2.61	49.83	9.86	17.12	23.19
CrSiC(10)	1.79	73.13	1.96	24.91	–
CrSiC(20)	1.80	68.75	3.46	27.79	–
CrSiC(30)	1.71	66.07	7.38	26.55	–

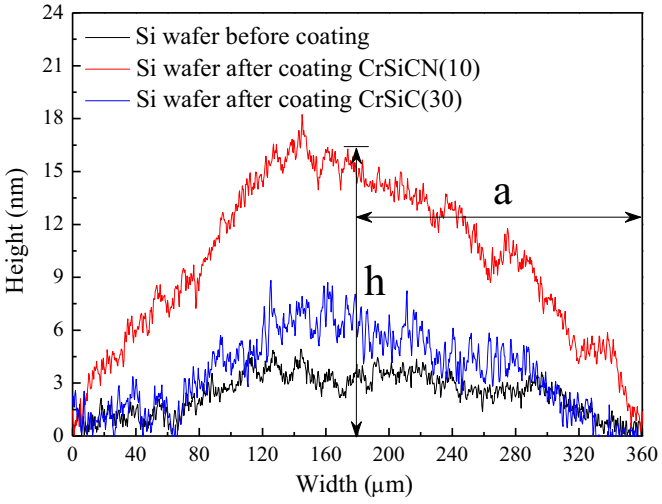

Fig. 1. Cross-section profiles of Si wafers before and after coating CrSiCN(10) and CrSiC(30).

2.2. Phase and residual stress of coatings

The thickness and element concentration of coatings were measured by field emission scanning electron microscope (FE-SEM) (JEOL-JSM-7001F and FEI-SIRION 200), and the results are listed in Table 1. The crystal structure of coatings was characterized by X-ray diffraction spectrum (D8-Advance, Bruker, Germany) with Cu Kα radiation (λ=0.15404 nm) at input voltage (40 kV) and current (40 mA). 2θ data was recorded from 30° to 80° with sampling pitch of 0.01 and scan rate of 10°/min. The cross-section profiles of Si wafers before and after coating, as well as roughness (Gaussian filter, 0.08 mm), were measured by white-light interferometer (CCI 3D, Taylor Hobson Ltd. UK). In here, only contours of CrSiCN(10) and CrSiC(30) coatings are illustrated in Fig. 1 to present the upward bending phenomenon, which is a typical result caused by compressive stress (σ). After the height (h) and width ($2a$) of each contour were measured, individual compressive stress (σ) of coatings could be calculated by Stoney's equation, which has been described in Ref. [38].

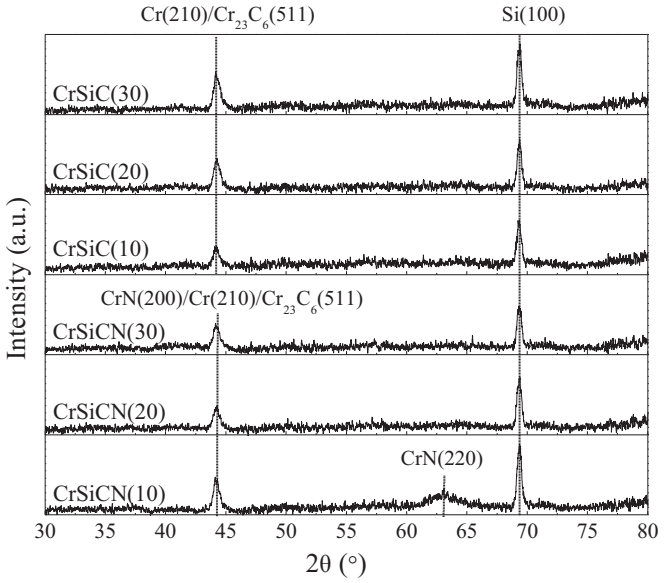

Fig. 2. X-ray diffraction spectra of CrSiCN and CrSiC coatings at different TMS flows.

Table 2
Mechanical properties of CrSiCN and CrSiC coatings at different TMS flows.

Coatings	H (GPa)	SD_H (GPa)	E (GPa)	SD_E (GPa)	H/E	H^3/E^2 (GPa)	W_e (%)	σ (GPa)	d/h
CrSiCN(10)	19.1	2.96	301	31.0	0.063	0.077	55.96	−4.67	0.81
CrSiCN(20)	13.1	0.87	251	11.5	0.052	0.036	47.41	−2.57	0.88
CrSiCN(30)	13.1	0.40	231	6.1	0.057	0.042	48.69	−1.52	0.70
CrSiC(10)	13.8	0.80	271	10.5	0.051	0.036	42.66	−1.71	1.00
CrSiC(20)	13.2	0.64	271	10.6	0.049	0.031	43.49	−1.64	1.00
CrSiC(30)	13.6	1.67	262	19.4	0.052	0.037	44.41	−1.18	1.05

Download English Version:

https://daneshyari.com/en/article/7977394

Download Persian Version:

https://daneshyari.com/article/7977394

Daneshyari.com